CHEMISTRY OF MATERIALS
Article

Chem. Mater. **2010,** *22,* 1595–1605 1595
DOI:10.1021/cm902784r

Cleavage Energy of Alkylammonium-Modified Montmorillonite and Relation to Exfoliation in Nanocomposites: Influence of Cation Density, Head Group Structure, and Chain Length

Yao-Tsung Fu and Hendrik Heinz*

Department of Polymer Engineering, University of Akron, Akron, Ohio 44325

Received September 6, 2009. Revised Manuscript Received December 30, 2009

Cohesion between layers of organically modified aluminosilicates creates a barrier to exfoliation in polymer matrices and can be thermodynamically described by the cleavage energy. While the measurement of cleavage energies at the nanometer scale is experimentally challenging, molecular simulation indicates a tunable range between 25 and 210 mJ/m^2 upon variation of the cation exchange capacity (CECs of 91 meq/100 g and 143 meq/100 g), headgroup chemistry (primary and quaternary ammonium), and chain length (C_2 to C_{22}) in a series of 44 alkylammonium-modified montmorillonites. Designed organoclays of low cleavage energy can support exfoliation when the surface tension, which relates to reconstructed surfaces after cleavage, is comparatively higher. The difference between high and low cleavage energies is associated with Coulomb interactions depending on the position of the positively charged surfactant head groups in the interlayer with respect to the two clay layers at equilibrium separation and further with the interlayer density depending on volume packing of the surfactants in the solvent-free minerals. Surfactants with NH_3 head groups exhibit low cleavage energies between 25 and 55 mJ/m^2. Surfactants with NMe_3 head groups exhibit cleavage energies up to 210 mJ/m^2 for short chain length and approach a range between 30 and 65 mJ/m^2 for longer alkyl chains. The cleavage energy as a function of chain length indicates local minima for interlayer structures comprised of loosely packed, flat-on layers of alkyl chains and local maxima for interlayer structures comprised of densely packed, flat-on layers of alkyl chains, convergent to 45 ± 5 mJ/m^2 for longer chains ($> C_{20}$). We employed molecular dynamics simulation in full atomistic detail using an accurate, extensively validated force field [Heinz et al. *Chem. Mater.* **2005**, *17*, 5658] and advanced sampling techniques to obtain equilibrium surfactant conformations.

1. Introduction

Layered silicates play an important role in the synthesis and processing of polymer nanocomposites, biodegradable hybrid materials, and cosmetics.[1−6] To achieve better compatibility with hydrophobic organic matrices, superficial alkali cations in hydrophilic minerals such as muscovite mica and montmorillonite can be exchanged for alkylammonium surfactants or other amphiphilic surfactants which transform the surface polarity from hydrophilic to hydrophobic.[7−11] The surface-modified layered silicates can often be better dispersed in synthetic and biological polymers and contribute to a broad range of functionality. For example, higher modulus and tensile strength, and heat resistance[12−14] as well as decreased gas permeability and flammability[15] were reported for nanocomposites in comparison to the neat polymer. A major challenge, however, is the exfoliation of the aluminosilicate layers in polymer matrices to create a bulk material of interfaces as opposed to intercalation or agglomeration of the layered silicates in the matrix.

Many approaches have been explored to achieve exfoliation, including the use of different minerals, variation in cation exchange capacity (CEC), surfactant architecture and chemistry, in situ polymerization of polymer precursors under addition of organically modified minerals, reactions between modified minerals and

*Corresponding author e-mail: hendrik.heinz@uakron.edu.

(1) *An Introduction to Clay Colloidal Chemistry*; Van Olphen, H., Wiley: New York, 1977.
(2) Usuki, A.; Kojima, Y.; Kawasumi, M.; Okada, A.; Fukushima, Y.; Kurauchi, T.; Kamigaito, O. *J. Mater. Res.* **1993**, *8*, 1179–1184.
(3) Messersmith, P. B.; Giannelis, E. P. *Chem. Mater.* **1994**, *6*, 1719–1725.
(4) Strawhecker, K. E.; Manias, E. *Chem. Mater.* **2000**, *12*, 2943–2949.
(5) Ray, S. S.; Yamada, K.; Okamoto, M.; Ueda, K. *Nano Lett.* **2002**, *2*, 1093–1096.
(6) Ray, S. S.; Okamoto, M. *Prog. Polym. Sci.* **2003**, *28*, 1539–1641.
(7) Osman, M. A.; Seyfang, G.; Suter, U. W. *J. Phys. Chem. B* **2000**, *104*, 4433–4439.
(8) Osman, M. A.; Ernst, M.; Meier, B. H.; Suter, U. W. *J. Phys. Chem. B* **2002**, *106*, 653–662.
(9) Heinz, H.; Castelijns, H. J.; Suter, U. W. *J. Am. Chem. Soc.* **2003**, *125*, 9500–9510.
(10) Osman, M. A.; Ploetze, M.; Skrabal, P. *J. Phys. Chem. B* **2004**, *108*, 2580–2588.
(11) Zhu, J. X.; He, H. P.; Zhu, L. Z.; Wen, X. Y.; Deng, F. *J. Colloid Interface Sci.* **2005**, *286*, 239–244.
(12) Vaia, R. A.; Teukolsky, R. K.; Giannelis, E. P. *Chem. Mater.* **1994**, *6*, 1017–1022.
(13) Vaia, R. A.; Giannelis, E. P. *Macromolecules* **1997**, *30*, 7990–7999.
(14) Vaia, R. A.; Giannelis, E. P. *Macromolecules* **1997**, *30*, 8000–8009.
(15) Osman, M. A.; Rupp, J. E. P.; Suter, U. W. *J. Mater. Chem.* **2005**, *15*, 1298–1304.

Published on Web 01/12/2010

polymer precursors followed by polymerization, and various extrusion techniques of mineral-filled polymer melts.[6−17] It has been possible to achieve exfoliation for specific systems; however, widely applicable and cost-effective approaches to exfoliate layered silicates in common hydrophobic and polar polymer matrices remain of great significance for automotive, aerospace, packaging, and commodity applications.

In spite of theoretical studies on clay minerals and polymers,[18−38] difficulties to achieve exfoliation in polymers using existing techniques are still linked to limited understanding of dispersion and self-assembly processes. The monitoring of exfoliation free energies at buried interfaces in polymer matrices is experimentally almost impossible and computationally demanding using accurate all-atom models. Nevertheless, the structural properties of self-assembled alkylammonium surfactants on montmorillonite surfaces have been understood at the molecular level[19,20,22−24,26,28−36] in quantitative agreement with X-ray, IR, SFG, NMR, NEXAFS, DSC, TGA, and TEM data,[7−15] including headgroup-surface interactions, gallery spacing, interlayer density, chain conformation, and thermal transitions. Molecular simulation also provided the first quantitative analysis of cleavage energies and surface reconstruction in mica,

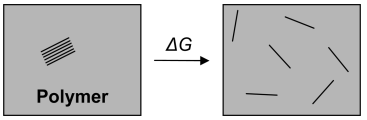

Figure 1. Schematic representation of exfoliation of aluminosilicate layers silicate in a polymer matrix.

montmorillonite, and selected organically modified minerals.[31] The separation of layered silicates is a critical process for dispersion in a matrix and large differences in cleavage energy are known depending on surface modification.[31,39,40] A limitation in experimental studies of nanocomposites has also been the use of a narrow range of surfactants with typical chain lengths between C_{14} and C_{18} which exploits only a fraction of the rich variety of possible interlayer environments.[7,8,10,12,33,35]

Therefore, this paper introduces a suitable thermodynamic model of the dispersion process and aims at a comprehensive analysis of cleavage energies and accompanying molecular-scale processes upon separation for a series of 44 modified montmorillonites. The series encompasses two different cation exchange capacities (91 and 143 meq/100 g), two head groups ($R-NH_3^+$ and $R-NMe_3^+$), and alkyl chains ranging from n-C_2H_5 to n-$C_{22}H_{45}$.

In section 2, we present the thermodynamic model for the dispersion of layered silicates in polymer matrices and discuss the role of cleavage energies and surface tensions. In section 3, we describe molecular models, force fields, and computational details. In section 4, we present the cleavage energies, their additive contributions, and molecular-level observations upon separation of the layers. Section 5 is dedicated to explaining the differences between computed cleavage energies and experimentally measured surface tensions and their effect on dispersion in a matrix. The paper concludes with a summary in section 6.

2. Thermodynamic Model for Dispersion of Layered Silicates in Polymer Matrices

2.1. Thermodynamic Considerations. During dispersion in a polymer matrix, the minerals (M) give up their cohesive free energy ΔG_M which equals the free energy of cleavage,[31] the polymer (P) gives up locally its cohesive free energy per area ΔG_P, and the two components form a new interface (MP) associated with a free energy ΔG_{MP}. The process is schematically depicted in Figure 1, and the overall change in free energy ΔG is

$$\Delta G = \Delta G_M + \Delta G_P + \Delta G_{MP} \quad (1)$$

The first two terms are positive, the third negative. The advantage of this free energy model is the focus on dispersion aspects and the full inclusion of entropic effects of the polymer in the second and third term.[13,14] Under the assumption that all surfaces would be well-defined and do

(16) Yalcin, B.; Cakmak, M. *Polymer* **2004**, *45*, 6623–6638.
(17) Jacobs, J. D.; Koerner, H.; Heinz, H.; Farmer, B. L.; Mirau, P. A.; Garrett, P. H.; Vaia, R. A. *J. Phys. Chem. B* **2006**, *110*, 20143–20157.
(18) Teppen, B. J.; Rasmussen, K.; Bertsch, P. M.; Miller, D. M.; Schafer, L. *J. Phys. Chem. B* **1997**, *101*, 1579–1587.
(19) Hackett, E.; Manias, E.; Giannelis, E. P. *J. Chem. Phys.* **1998**, *108*, 7410–7415.
(20) Pospisil, M.; Capkova, P.; Merinska, D.; Malac, Z.; Simonik, J. *J. Colloid Interface Sci.* **2001**, *236*, 127–131.
(21) Kuppa, V.; Manias, E. *Chem. Mater.* **2002**, *14*, 2171–2175.
(22) Zeng, Q. H.; Yu, A. B.; Lu, G. Q.; Standish, R. K. *Chem. Mater.* **2003**, *15*, 4732–4738.
(23) Pospisil, M.; Kalendova, A.; Capkova, P.; Simonik, J.; Valaskova, M. *J. Colloid Interface Sci.* **2004**, *277*, 154–161.
(24) Heinz, H.; Paul, W.; Binder, K.; Suter, U. W. *J. Chem. Phys.* **2004**, *120*, 3847–3854.
(25) Gournis, D.; Georgakilas, V.; Karakassides, M. A.; Bakas, T.; Kordatos, K.; Prato, M.; Fanti, M.; Zerbetto, F. *J. Am. Chem. Soc.* **2004**, *126*, 8561–8568.
(26) Zeng, Q. H.; Yu, A. B.; Lu, G. Q.; Standish, R. K. *J. Phys. Chem. B* **2004**, *108*, 10025–10033.
(27) Pandey, R. B.; Anderson, K. L.; Heinz, H.; Farmer, B. L. *J. Polym. Sci., Part B* **2005**, *43*, 1041–1046.
(28) Greenwell, H. C.; Harvey, M. J.; Boulet, P.; Bowden, A. A.; Coveney, P. V.; Whiting, A. *Macromolecules* **2005**, *38*, 6189–6200.
(29) He, H. P.; Galy, J.; Gerard, J. F. *J. Phys. Chem. B* **2005**, *109*, 13301–13306.
(30) Katti, K. S.; Sikdar, D.; Katti, D. R.; Ghosh, P.; Verma, D. *Polymer* **2006**, *47*, 403–414.
(31) Heinz, H.; Vaia, R.; Farmer, B. L. *J. Chem. Phys.* **2006**, *124*, 224713.
(32) Gournis, D.; Jankovic, L.; Maccallini, E.; Benne, D.; Rudolf, P.; Colomer, J. F.; Sooambar, C.; Georgakilas, V.; Prato, M.; Fanti, M.; Zerbetto, F.; Sarova, G. H.; Guldi, D. M. *J. Am. Chem. Soc.* **2006**, *128*, 6154–6163.
(33) Heinz, H.; Vaia, R. A.; Krishnamoorti, R.; Farmer, B. L. *Chem. Mater.* **2007**, *19*, 59–68.
(34) Fermeglia, M.; Pricl, S. *Prog. Org. Coat.* **2007**, *58*, 187–199.
(35) Heinz, H.; Vaia, R. A.; Farmer, B. L. *Langmuir* **2008**, *24*, 3727–3733.
(36) Heinz, H.; Vaia, R. A.; Koerner, H.; Farmer, B. L. *Chem. Mater.* **2008**, *20*, 6444–6456.
(37) Cygan, R. T.; Greathouse, J. A.; Heinz, H.; Kalinichev, A. G. *J. Mater. Chem.* **2009**, *19*, 2470–2481.
(38) Suter, J. L.; Anderson, R. L.; Greenwell, H. C.; Coveney, P. V. *J. Mater. Chem.* **2009**, *19*, 2482–2493.
(39) Giese, R. F. *Nature* (*London*) **1974**, *248*, 580–581.
(40) Adamson, A. W.; Gast, A. P. *Physical Chemistry of Surfaces*, 6th ed.; Wiley: New York, 1997; Chapter VII.

not reconstruct, eq 1 can be rewritten per interfacial area using surface and interface tensions

$$\gamma_{MP} = \gamma_M + \gamma_P + \Delta G_{MP} \quad (2)$$

γ_{MP} reflects the definition of the mineral-polymer interface tension,[41−45] whether or not eq 2 could be a substitute for eq 1. For example, if the two components M and P were identical ($\gamma_M = \gamma_P$), the recombination $\Delta G_{MP} = -2\gamma_M = -2\gamma_P$ recovers the separation free energy, and the interface tension γ_{MP} would equal zero. When the two components are different, most but not all of the separation energies γ_M and γ_P can typically be recovered by ΔG_{MP} so that a small positive interface tension γ_{MP} results. Under the assumption that all surfaces would be ideal, this small positive term thermodynamically represents the agglomeration of mineral components in polymer matrices.

In a real system, however, neither the mineral, the polymer, nor the mineral-(surfactant-)polymer interface are ideal, i.e., all surfaces are typically irregular and significantly reconstruct upon dispersion. Therefore, a thermodynamically spontaneous process requires $\Delta G < 0$ according to eq 1, and γ_{MP} according to eq 2 may have a very different value. However, we can expand eq 1 using eq 2 simply as a definition of ΔG_{MP}

$$\begin{aligned}\Delta G &= \Delta G_M + \Delta G_P + \Delta G_{MP} \\ &= \Delta G_M - \gamma_M + \Delta G_P - \gamma_P + \gamma_{MP}\end{aligned} \quad (3)$$

Equation 3 can be employed to describe the dispersion process and shows how differences between cleavage free energy and surface tension as well as the interface tension determine the exfoliation free energy ΔG.

For example, the high cleavage energy of natural minerals, such as $\Delta G_M = 130$ mJ/m^2 in montmorillonite (91 meq/100 g) as opposed to a surface tension γ_M near 60 mJ/m^2,[43] combined with typical cleavage free energy (∼surface tension) of polymers ΔG_P between 20 and 60 mJ/m^2 result in a high positive value of ΔG (+70 mJ/m^2 + γ_{MP}) which prevents exfoliation. In contrast, common surfactants such as in octadecylammonium montmorillonite[31,43] lower ΔG_M to about 40 mJ/m^2, and the surface tension γ_M is of similar value.[43] Then, ΔG will be significantly smaller ($\sim\gamma_{MP}$) although it often remains greater than zero which represents experimentally observed agglomeration. When a typically positive interface tension remains, it can only be lowered to negative exfoliation energies by cleavage free energies of the components lower than the respective surface tensions (see eq 3). In conclusion, the process may be driven in favor of exfoliation by three options: lower ΔG_M, lower ΔG_P, or lower ΔG_{MP} as explained in the following.

2.2. Methods To Lower the Free Energy of Exfoliation ΔG. In this paper, we survey values of ΔG_M which is closely approximated by the cleavage energy.[31] A reduction in cleavage free energy ΔG_M would result in a higher propensity of exfoliation of the organically modified clay mineral layers in polymer matrices, assuming that the interfacial free energy ΔG_{MP} upon interaction with the polymer increases to a lesser extent (eq 1). It has been shown that ΔG_{MP} is approximately the same for modified minerals with low ΔG_M and for natural minerals of up to 100 times higher ΔG_M (mica)[39,40,42,43] as the attraction of organic matter to the final cleaved mineral surface does not significantly change whether the surface consists of surfactants or cations. This suggests that surfactant-modified minerals of particularly low cleavage energy ΔG_M, e.g., due to minimal interlayer density, would still yield a similar value of ΔG_{MP} after cleavage and thus offer a pathway to a negative ΔG.

Alternatively, a decrease in ΔG_P and in ΔG_{MP} (eq 1) can increase the propensity of exfoliation. A lower cohesive free energy per area of the polymer ΔG_P (low surface tension) imposes conditions on the polymer and narrows down choices for a wide range of functional composites. Therefore, this approach is less desirable. A lower ΔG_P would be furthermore effective in increasing dispersion only if the (negative) free energy of formation of the mineral-polymer interface ΔG_{MP} can be sustained or increases less than ΔG_P decreases.

The third term, ΔG_{MP}, can be lowered by reactions between functionalized surfactants and the polymer. This option is a powerful, proven way to achieve dispersion; however, it requires the use of more expensive functionalized surfactants. Similarly, other attractive interactions such as hydrogen bonds and multipole Coulomb forces between mineral, surfactant, and polymer lower ΔG_{MP}, although in this case the gain during interface formation will often be compensated by higher cleavage free energies of the modified mineral ΔG_M and of the neat polymer ΔG_P so that no net reduction in the free energy of exfoliation ΔG results (eq 1).

2.3. Cleavage Energy and Surface Tension. The free energy of cleavage ΔG_M is thus a suitable parameter to tune the free energy of exfoliation ΔG. The difference between the cleavage free energy and the surface tension (eq 3) lies in reconstruction of the surface during cleavage. For example, ΔG_M may vary between slow (equilibrium) and fast (nonequilibrium) cleavage,[40] it can be very high when interlayer cations are separated upon cleavage,[31] and it can differ for densely and loosely packed alkyl chains between the layers. Therefore, it is distinct from the surface tension which is determined for surfaces after cleavage in contact with different liquids.[31] The cleavage free energy and the surface tension can be similar, however, when surfaces undergo minimal reconstruction upon cleavage or when they undergo similar reconstruction processes upon cleavage as they undergo upon interaction with liquids during contact angle measurements.

(41) Van Oss, C. J.; Chaudhury, M. K.; Good, R. J. *Chem. Rev.* **1988**, *88*, 927–941.
(42) *Organo-Clay Complexes and Interactions*; Yariv, S., Cross, H., Eds.; Dekker: New York, 2002.
(43) Giese, R. F.; Van Oss, C. J. *Colloid and Surface Properties of Clays and Related Minerals*; Dekker: New York, 2002.
(44) Lewin, M.; Mey-Marom, A.; Frank, R. *Polym. Adv. Tech.* **2005**, *16*, 429–441.
(45) Kamal, M. R.; Calderon, J. U.; Lennox, R. B. *J. Adhes. Sci. Technol.* **2009**, *23*, 663–688.

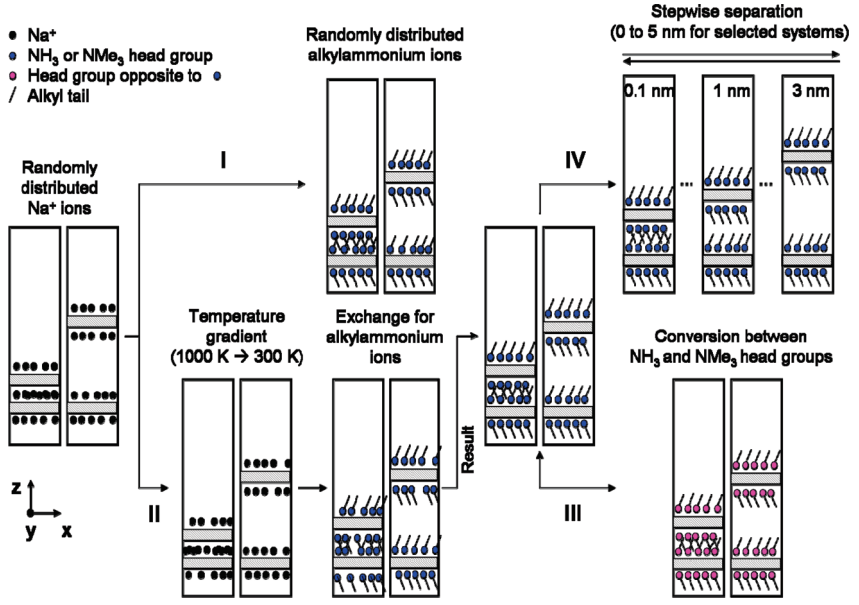

Figure 2. Four methods to compute the cleavage energy of two organically modified montmorillonite layers. In method I, alkylammonium ions replace a random distribution of alkali ions on the surface of montmorillonite, and the system is subjected to molecular dynamics (MD) relaxation. In method II, a redistribution of alkali ions (or ammonium ions) is generated using MD with a temperature gradient, followed by alkylammonium substitution and subsequent MD relaxation. In method III, the headgroup composition is changed using the results from method II, and the structures are subjected to MD relaxation again. In method IV, MD relaxation is performed for stepwise increasing separation of the layers (using constraints) starting with the results of method II. Every method yields an average energy for unified and cleaved montmorillonite layers. The comparison of these values allows the identification of energetically preferred conformations in each state, the computation of the cleavage energy, and an estimate of the uncertainty.

We define the cleavage energy ε_S (focusing on the energy contribution only) per contact surface area $2A$ as the difference in average total energy between a cleaved assembly of layers at infinite separation ΔE_S and the united assembly of layers at equilibrium distance ΔE_U, assuming a slow cleavage process in thermodynamic equilibrium[31]

$$\varepsilon_S = \frac{\Delta E_S - \Delta E_U}{2A} \tag{4}$$

The cleavage energy ε_S approximates the surface tension when surface reconstruction and changes in entropy upon cleavage are minimal. In these cases, cleavage energies can be related to contact angle measurements, thin-layer wicking, and other surface data;[39−45] however, the processes to which the data are related in experiment and in the simulation must be carefully examined.

3. Computational Models and Methods

3.1. Models. We consider two common montmorillonites of the formulas $Na_{0.333}[Si_4O_8][Al_{1.667}Mg_{0.333}O_2(OH)_2]$ and $Na_{0.533}[Si_4O_8][Al_{1.467}Mg_{0.533}O_2(OH)_2]$ which correspond to the cation exchange capacity (CEC) of 91 meq/100 g and 143 meq/100 g, respectively. These compositions approximate natural montmorillonite from Southern Clay Products and Nanocor clay, respectively.[33] Initial structures were derived from X-ray data[46−50] as a $5 \times 3 \times 1$ multiple of the unit cell, and the distribution of $AlO(OH) \rightarrow MgO(OH)^- \cdots Na^+$ charge defects follows solid state NMR data.[51,52]

Models of the alkylammonium surfactants of the type $N(CH_3)_3^+-C_nH_{2n+1}$ and $NH_3^+-C_nH_{2n+1}$ with chain lengths $n = 2, 4, 6, ..., 22$ (symbol C_2, C_4, ..., C_{22}) were prepared using the graphical interface of Materials Studio.[53]

Models of the modified montmorillonite structures were built by replacement of the alkali cations on a single layer of the natural montmorillonite by alkylammonium surfactants so that the center of the headgroup resides near the equilibrium position of the previous Na^+ ions, followed by molecular dynamics relaxation between 100 and 500 ps depending on chain length. All systems were contained in a cubic box of $2.596 \times 2.705 \times 22\ nm^3$ size, corresponding to a $5 \times 3 \times 1$ multiple of the unit cell of montmorillonite with periodic boundary conditions in the xy plane and essentially an open boundary in the z direction which allows free equilibration of the gallery spacing (Figure 2).[24] The structures are identical to the ones used in ref 33.

3.2. Force Field. We employed the phyllosilicate force field[51] embedded in the polymer consistent force field (PCFF).[53] This semiempirical model for layered silicates reproduces the surface energy, crystal structure, and vibration frequencies in very good agreement with experimental results, in contrast to other force field models.[18−22,25,29,34,38] The reproduction of surface and interface energies in this model is essential for the reliability of cleavage energies, binding energies, and miscibility predictions.[51] Atomic charges for the surfactant head groups were assigned according to the method of Heinz and Suter,[54]

(46) Rothbauer, R. *Neues Jahrb. Mineral., Monatsh.* **1971**, 143–154.
(47) Brown, G. *The X-ray Identification and Crystal Structures of Clay Minerals*; Mineralogical Society: London, 1961.
(48) *Reviews in Mineralogy*; Bailey, S. W., Ed.; Mineralogical Society of America: Chelsea, MI, 1988; Vol. *19*. See, also: http://www.webmineral.com.
(49) Lee, J. H.; Guggenheim, S. *Am. Mineral.* **1981**, *66*, 350–357.
(50) Tsipurski, S. I.; Drits, V. A. *Clay Miner.* **1984**, *19*, 177–193. Mg positions are not correct.
(51) Heinz, H.; Koerner, H.; Anderson, K. L.; Vaia, R. A.; Farmer, B. L. *Chem. Mater.* **2005**, *17*, 5658–5669.
(52) Heinz, H.; Suter, U. W. *Angew. Chem., Int. Ed.* **2004**, *43*, 2239–2243.
(53) *Materials Studio and Discover program, version 96.0/4.0.0*; Accelrys, Inc.: San Diego, CA, 2005.
(54) Heinz, H.; Suter, U. W. *J. Phys. Chem. B* **2004**, *108*, 18341–18352.

i.e., −0.1e for N and +0.275e for each C in CH_3 and CH_2 groups adjacent to N in $R-N(CH_3)_3^+$ as well as −0.5e for N, +0.4e for H, and +0.3e for C in the CH_2 group adjacent to N in $R-NH_3^+$.[33,51] PCFF includes reliable parameters for hydrocarbon chains as previously described.[9]

3.3. Advanced Sampling Techniques and Simulation Protocol. The simulation of cleaved and unified alkylammonium montmorillonites was carried out for every system using several approaches to identify thermodynamically stable arrangements of the surfactants (Figure 2). The different equilibration schemes were developed for improved configuration sampling as relaxation times of the alkyl chains on the surface exceed typical simulation times of 1 ns. In addition, multiple simulations using structures with different initial orientation of the hydrocarbon tails and different initial positions of the head groups on the surface were essential. Using protocols I to IV (Figure 2) and several repetitions within each method improved the convergence and reduced error estimates for most systems to ± 3 mJ/m^2. The theoretically possible limit of accuracy might be < 0.5 mJ/m^2 although it is not currently feasible due to finite size effects associated with the distribution of charge defects and surfactants as well as the need for excessive computational resources.

In method I (Figure 2), sodium ions on a single montmorillonite layer were substituted by alkylammonium ions in random lateral positions so that head groups were approximately positioned at the same vertical distance from the surface as previous sodium ions. A total of 44 such structures were prepared (alkyl chains C_2, C_4, ..., C_{22}; NH_3 and NMe_3 head groups; CEC = 91 meq/100 g and CEC = 143 meq/100 g). The single layers were subjected to 200 ps molecular dynamics in the NVT ensemble, and the model was subsequently duplicated and further equilibrated for 400 ps using the Discover program.[40] The last snapshot of these duplicate structures (energy difference < 1 mJ/m^2) was chosen as a start structure for equilibration of the unified assembly (E_U), and the corresponding two single layers served individually as start structures for equilibration of the separated assembly (E_{S1}, E_{S2}). All structures involved a separation of 8 nm along the z direction to the next periodic image. The duration of the molecular dynamics simulation was 200 to 600 ps in the NVT ensemble for further pre-equilibration and subsequently 400 to 800 ps to sample the average energy including Coulomb, van der Waals, and internal contributions. Thereby, longer simulation times were assigned to longer alkyl chains. The cleavage energy ε_S was calculated from the average energies E_U, E_{S1}, E_{S2} as $\varepsilon_S = (E_{S1} + E_{S2} - E_U)/(2A)$ according to eq 4. The procedure was repeated for up to 5 independent pairs of structures for each of the 44 systems to improve statistics.

In method II (Figure 2), sodium or ammonium ions in random position on the surface of unified and cleaved montmorillonite layers were subjected to 10 ps NVT dynamics using a steep temperature gradient from 10000 to 298 K, while coordinates of all other atoms were fixed (Berendsen thermostat with a decay constant of 1 ps). This allowed the alkali ions to move laterally across superficial cavities and locate favorable energy minima. The temperature gradient procedure was repeated five times with different initial distribution of the sodium or ammonium ions to identify the equilibrium distribution (uncertainty < 5 mJ/m^2). For the unified and cleaved structure of lowest energy, sodium or ammonium ions were subsequently replaced by alkylammonium ions to generate 44 pairs of different systems whereby the ammonium head groups occupied the former positions of the sodium/ammonium ions. The surfactant-modified structures were initially subjected to ~200 ps molecular dynamics in the NVT ensemble to relax the orientation of the alkyl tails, 200 to 600 ps for equilibration, and 400 to 800 ps for data recording.

In method III (Figure 2), the final snapshots of all 44 pairs of assemblies from method II were employed to replace NH_3 head groups by NMe_3 head groups or NMe_3 head groups by NH_3 head groups, respectively. Subsequently, the structures with exchanged head groups were subjected to ~200 ps NVT molecular dynamics for initial relaxation, 200 to 600 ps for equilibration, and 400 to 800 ps to record average total energies, Coulomb, van der Waals, and internal contributions.

In method IV (Figure 2), the cleavage energy of the duplicate assemblies was computed as a function of stepwise separation in the intervals 0, 0.01, 0.03, 0.05, 0.1, 0.3, 0.5, 1, 1.5, 2, 3, and 5 nm. An average final structure from method II served as an input at 0 nm separation. No changes in energy were found beyond 3 nm separation within an uncertainty of ± 1 mJ/m^2.[31] One hundred ps molecular dynamics were carried out at every step. To maintain a constant separation at a given interval, all atoms different from alkylammonium surfactants were spatially constrained during the simulation. The cleavage energy was computed as the difference between the average total energy at 5 nm separation and at 0 nm separation, including additive contributions. Method IV was time-consuming and only applied to the 11 systems in the CEC 91 meq/100 g, $N(CH_3)_3$-C_nH_{2n+1} series.

Molecular dynamics simulations were carried out using the LAMMPS[55] and Discover[53] programs. The programs perform equivalent tasks whereby LAMMPS uses shorter simulation time and Discover is better integrated in a graphical environment for visualization. Computed total energies agree within < 1 kcal/mol, and energy differences relevant for the computation of cleavage energies agree within < 0.1 kcal/mol (< 0.05 mJ/m^2) for the same system. The NVT ensemble, the Verlet integrator, a time step of 1 fs, and a temperature of 298.15 K were chosen. Temperature control was facilitated by a Nose/Hoover thermostat (LAMMPS) and the Anderson thermostat (Discover), respectively. A spherical cutoff at 1.2 nm was employed for van der Waals interactions, and Coulomb interactions were evaluated using a particle−particle particle-mesh solver (LAMMPS) and Ewald summation (Discover), both with very high accuracy (10^{-6} kcal/mol).

3.4. Analysis. Cleavage energies were computed according to eq 4 as the energy difference between cleaved and unified systems in relation to two times the lateral cross-sectional area of the box which equals the surface area $2A$. The average total energy in the cleaved and in the unified state was obtained by analysis of the results of independent simulations for each of the methods I to IV, aiming at the identification of the global energy minimum in the complex energy landscape. For this purpose, the method leading to the lowest average total energy was assigned the highest weight, and partial weight was assigned to other methods leading to energies near the global minimum. Changes in the assignment of these weights provided a measure of the uncertainty (see the Supporting Information for details). The total cleavage energy consists of additive contributions from internal energy (bond stretching, angle bending, torsion), Coulomb energy, van der Waals energy, and kinetic energy. The contribution of the kinetic energy was zero in all systems due to constant temperature with negligible deviations in the NVT ensemble. Visual inspection of the MD trajectories provided

(55) Plimpton, S. J. J. Comput. Phys. **1995**, *117*, 1−19. See, also: www.lammps.sandia.gov.

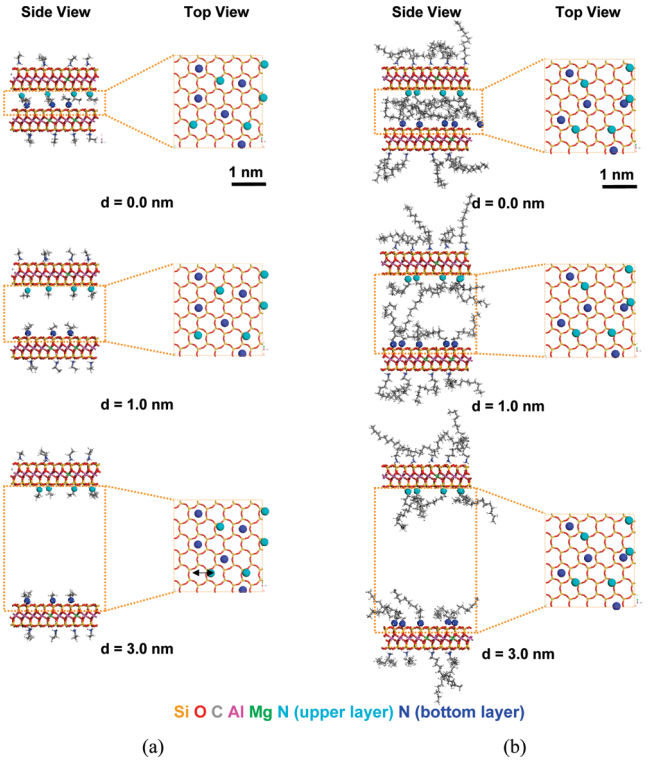

Figure 3. Snapshots of (a) $C_2H_5-NH_3^+$ surfactants and (b) $C_{14}H_{29}-NH_3^+$ surfactants at low CEC (91 meq/100 g) as a function of layer separation *d*. Lateral rearrangements of ammonium head groups are rarely found, indicated by the arrow. Projections in the *xz* plane (side view) and in the *xy* plane (top view) are shown. The vertical distribution of the ammonium head groups between the two montmorillonite layers at $d = 0$ nm for short surfactants in (a) as well as for longer surfactants in (b) leads to the absence of significant Coulomb contributions to the cleavage energy.

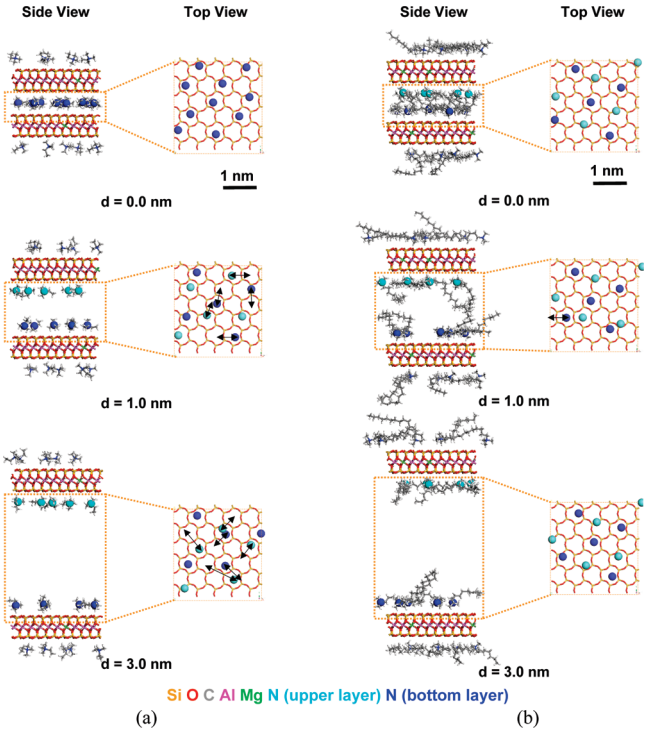

Figure 4. Snapshots of (a) $C_2H_5-N(CH_3)_3^+$ surfactants and (b) $C_{14}H_{29}-N(CH_3)_3^+$ surfactants at low CEC (91 meq/100 g) as a function of layer separation *d*. Lateral rearrangements of ammonium head groups are indicated by arrows and registered more frequently for short C_2 chains. Projections in the *xz* plane (side view) and in the *xy* plane (top view) are shown. Vertical sharing of the trimethylammonium head groups between the two montmorillonite layers at $d = 0$ nm for the short surfactants in (a) leads to strong Coulomb contributions to the cleavage energy in contrast to the longer surfactants in (b).

insight into interactions of the head groups with the surface and into surface reconstruction.

The existence of various local energy minima of the organically modified clay minerals in the simulation leads to an uncertainty in cleavage energy among single independent trajectories using method I between ±5 and ±10 mJ/m^2 for all models. Additional calculations using method I with 3 to 5 different start structures reduced this uncertainty; however, further computations using methods II, III, and IV (Figure 2) were essential to identify the most stable unified and cleaved structures along with a reduction of the uncertainty in cleavage energy to between ±2 and ±5 mJ/m^2.

4. Results and Discussion

Cleavage of alkylammonium montmorillonites involves the separation of the organic layers and lateral movement (diffusion) of the surfactants on the surface. In the solvent-free state considered in the simulation, the lateral mobility is lower for primary alkylammonium ions due to the formation of hydrogen bonds and proximity to the superficial cavities in the [Si,O] 12-rings on the surface (Figures 3 and 5). The mobility is higher for NMe_3 head groups due to the lack of hydrogen bonds and larger distance of the N atom from the montmorillonite surface (Figures 4 and 6).[33] We also observe a decrease in mobility for either type of headgroup with increasing chain length (Figures 3, 4, 5, 6). The main influence of higher CEC (Figures 5 and 6) in comparison to lower CEC (Figures 3 and 4) consists in an increased gallery spacing and increasingly hydrocarbon-like behavior of the interlayer.

These features allow a systematic understanding of cleavage energies as a function of CEC, headgroup chemistry, and chain length which is graphically depicted in Figure 7. A striking observation is the higher cleavage energy of short quaternary alkylammonium surfactants versus the consistently lower cleavage energy of primary alkylammonium surfactants. This distinction arises from differences in vertical distribution of the cationic head groups between the layers at equilibrium separation. Bulky quaternary ammonium head groups are located in the vertical center of the interlayer for short chain lengths (Figures 4 and 6) which leads to strongly attractive Coulomb interactions between each quaternary cation and anionic defect sites in both clay layers and some opposing repulsion by cation neighbors in the interlayer. Similar to unmodified clay minerals,[31] the cleavage energy is then very high and decreases only after a partial second alkyl layer causes the head groups to vertically separate between the layers, thereby breaking the strong Coulomb attraction across the interlayer (C_{14} in Figures 4 and 6). Thus, the cleavage energy of montmorillonite with quaternary alkylammonium ions decreases at a chain length equivalent to a partial alkyl bilayer (Figure 7).

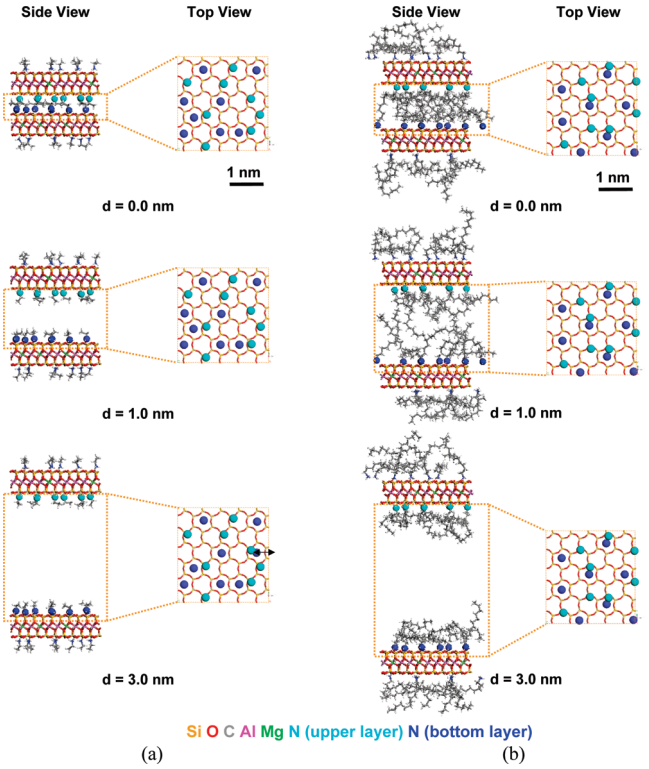

Figure 5. Snapshots of (a) $C_2H_5-NH_3^+$ surfactants and (b) $C_{14}H_{29}-NH_3^+$ surfactants at high CEC (143 meq/100 g) as a function of layer separation *d*. Lateral rearrangements of ammonium head groups are rarely found, indicated by arrows. Projections in the *xz* plane (side view) and in the *xy* plane (top view) are shown. The vertical distribution of the ammonium head groups between the two montmorillonite layers at $d = 0$ nm for the short surfactants in (a) as well as for the longer surfactants in (b) leads to the absence of significant Coulomb contributions to the cleavage energy.

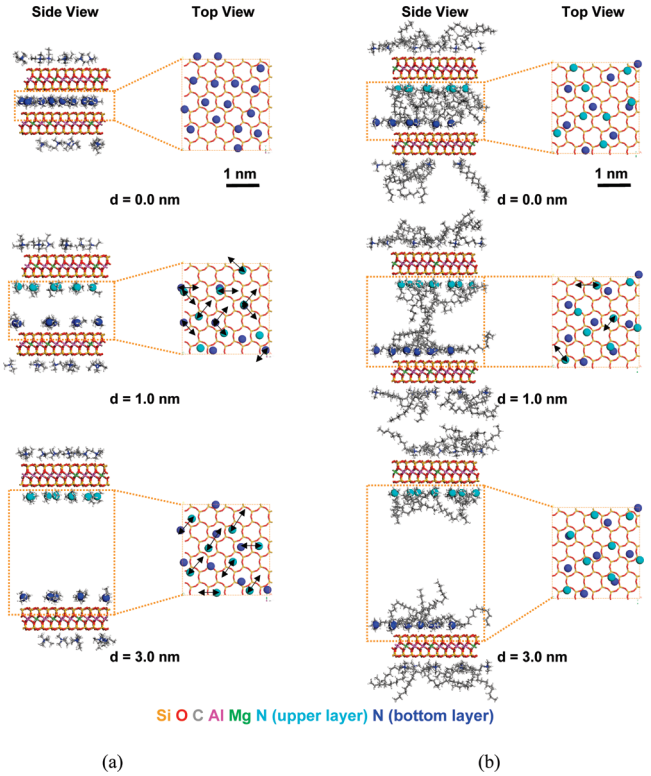

Figure 6. Snapshots of the conformation of (a) $C_2H_5-N(CH_3)_3^+$ surfactants and (b) $C_{14}H_{29}-N(CH_3)_3^+$ surfactants at high CEC (143 meq/100 g) as a function of layer separation *d*. Lateral rearrangements of ammonium head groups are indicated by arrows and registered more frequently for C_2 surfactants than for C_{14} surfactants. Projections in the *xz* plane (side view) and in the *xy* plane (top view) are shown. Vertical sharing of the trimethylammonium head groups between the two montmorillonite layers at $d = 0$ nm for the short surfactants in (a) leads to strong Coulomb contributions to the cleavage energy in contrast to the longer surfactants in (b).

In the case of primary alkylammonium ions, head groups are vertically separated between the two layers even for the shortest surfactants due to their small size and strong binding to the surface of only one clay layer supported by hydrogen bonds (C_2 in Figures 3 and 5).[33] Thus Coulomb interactions across the interlayer are then so much reduced that the cleavage energy is mostly determined by van der Waals interactions between the short alkyl chains and changes periodically with the formation of densely packed and loosely packed alkyl layers (Figure 7).

In particular, the distinctively low cleavage energies for montmorillonite modified with short primary ammonium ions are a novel result as they would greatly support exfoliation in polymer matrices by lowering ΔG_M as discussed in section 2 (eq 3). Details of this interesting behavior, including the breakdown of the total separation energy into Coulomb, van der Waals, and remaining contributions will be presented and explained in the following.

4.1. Alkylammonium Montmorillonite of Low CEC. A low CEC of 91 meq/100 g corresponds to 0.71 cations per nm^2 on a single montmorillonite even surface and to a nominal packing density $\lambda_0 = 0.13$ of the alkyl chains.[35] Figure 8 shows the cleavage energies and the additive contributions from Coulomb, van der Waals, and internal energy.

For surfactants with NH_3 head groups (Figure 8a), the cleavage energy follows a trend closely associated with packing of the alkyl layers in the interlayer space. Lower cleavage energy is observed in loosely packed alkyl layers since less van der Waals interactions are removed across the interlayer space upon cleavage. Higher cleavage energy is observed in densely packed alkyl layers as more van der Waals interactions are removed across the interlayer space upon cleavage resulting. Lowest cleavage energies of 25 mJ/m^2 and 33 mJ/m^2 are computed for C_4 and C_{14} surfactants, corresponding to a loosely packed alkyl monolayer and a loosely packed alkyl bilayer in the interlayer space, respectively. Highest cleavage energies of 46 and 52 mJ/m^2 are seen for C_{10} (C_8) and C_{22} surfactants, corresponding to a densely packed alkyl monolayer and a densely packed alkyl bilayer in the interlayer space, respectively. A slightly increased value for C_2 surfactants arises from residual Coulomb interactions. The most remarkable difference to quaternary ammonium head groups is the small magnitude of Coulomb interactions < 20 mJ/m^2 due to the vertical distribution of head groups between the two montmorillonite layers at equilibrium separation. The attachment of the small primary, hydrogen-bonded head groups to either one of the two montmorillonite layers at equilibrium separation can be seen for both C_2 and C_{14} surfactants in Figure 3

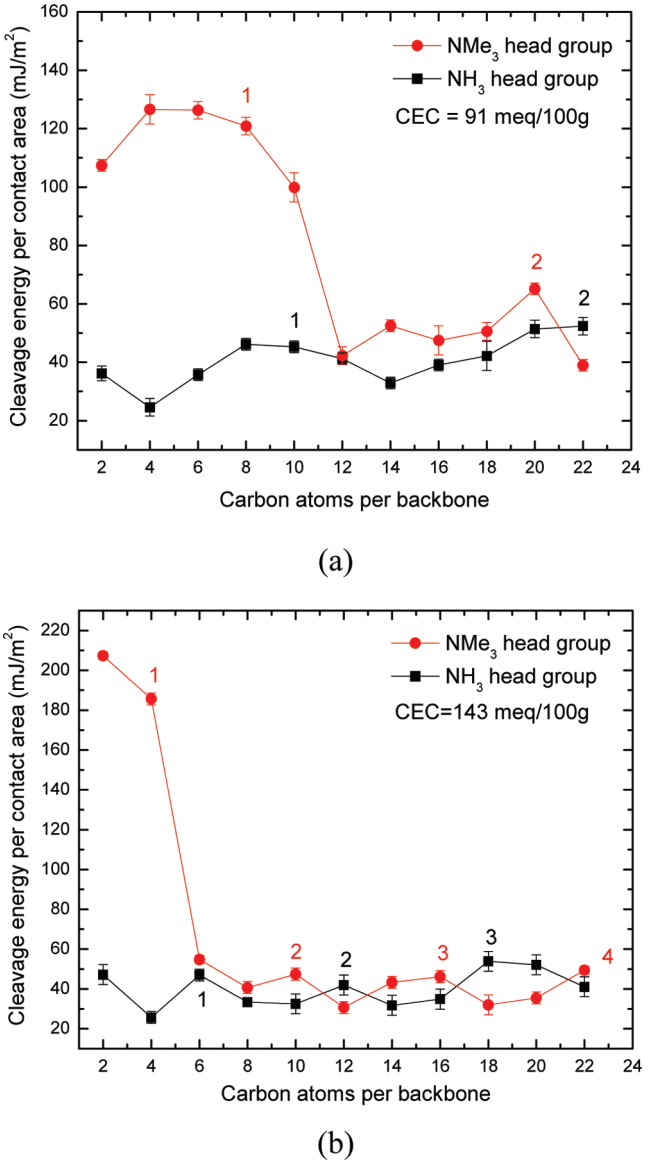

Figure 7. Cleavage energy of two montmorillonite layers modified with C_n-alkylammonium ions as a function of chain length n and headgroup structure (NH_3 and NMe_3). (a) Low CEC (91 meq/100 g) and (b) high CEC (143 meq/100 g). The labels 1, 2, 3, and 4 indicate the chain length at which a densely packed alkyl monolayer, bilayer, pseudotrilayer, and pseudoquadrilayer are formed in the interlayer space (ref 33).

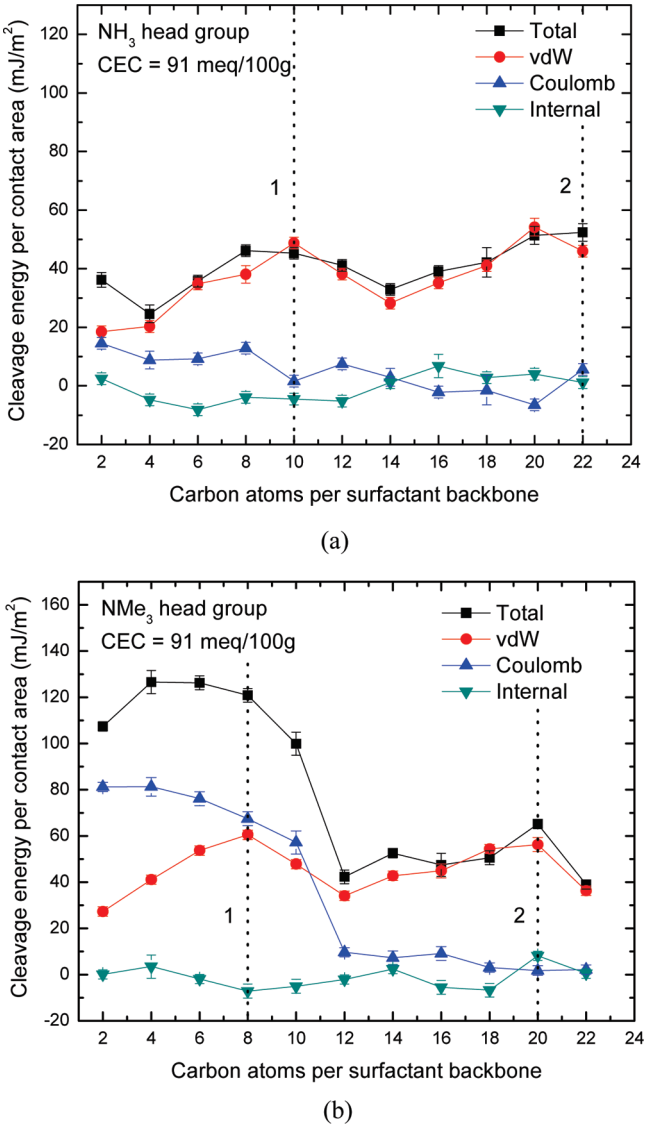

Figure 8. Cleavage energy and additive contributions from Coulomb, van der Waals, and internal interactions for montmorillonite of low CEC (91 meq/100 g) modified with (a) alkylammonium ions with NH_3 head groups and (b) alkylammonium ions with NMe_3 head groups. The vertical lines designated 1 and 2 indicate the chain length corresponding to a densely packed flat-on alkyl monolayer and a densely packed flat-on alkyl bilayer in the interlayer space.

(d = 0 nm). Residual Coulomb energy decreases with increasing chain length to minor values beyond C_8. The van der Waals energy increases steadily toward a densely packed alkyl monolayer at C_{10}, followed by a decrease for a partial alkyl bilayer and another increase toward a densely packed alkyl bilayer at C_{22}. The trend in cleavage energy follows approximately the trend in van der Waals contributions and the uncertainty is typically ± 3 mJ/m^2.

For surfactants with NMe_3 head groups (Figure 8b), the cleavage energy reaches a maximum near 126 mJ/m^2 for the chain length C_4 and C_6, goes through a minimum near 42 mJ/m^2 at C_{12}, reaches a second maximum of 65 mJ/m^2 at C_{20}, and falls to 39 mJ/m^2 at C_{22}. High cleavage energies for chain lengths up to a partial alkyl bilayer (C_{10}) result from significant Coulomb contributions up to 80 mJ/m^2 associated with vertical sharing of head groups between the two montmorillonite layers at equilibrium separation. The head groups separate vertically between the two layers upon formation of a partial alkyl bilayer in the interlayer space at chain length C_{12}, leading to a significant decrease in Coulomb energy. The difference in headgroup distribution is illustrated in Figure 4 for C_2 (no vertical separation at d = 0 nm) and C_{14} (vertical separation at d = 0 nm). The van der Waals contribution ranges between 27 mJ/m^2 and 60 mJ/m^2 and increases toward formation of a densely packed alkyl monolayer at C_8, decreases due to the formation of a partial alkyl bilayer with a minimum at C_{12}, and increases toward formation of a densely packed alkyl bilayer at C_{20}. The maximum cleavage energy of 126 mJ/m^2 between C_4 and C_6 arises from a superposition of Coulomb and van der Waals contributions (Figure 8b). The minimum of the cleavage energy at C_{12} is related to a low Coulomb

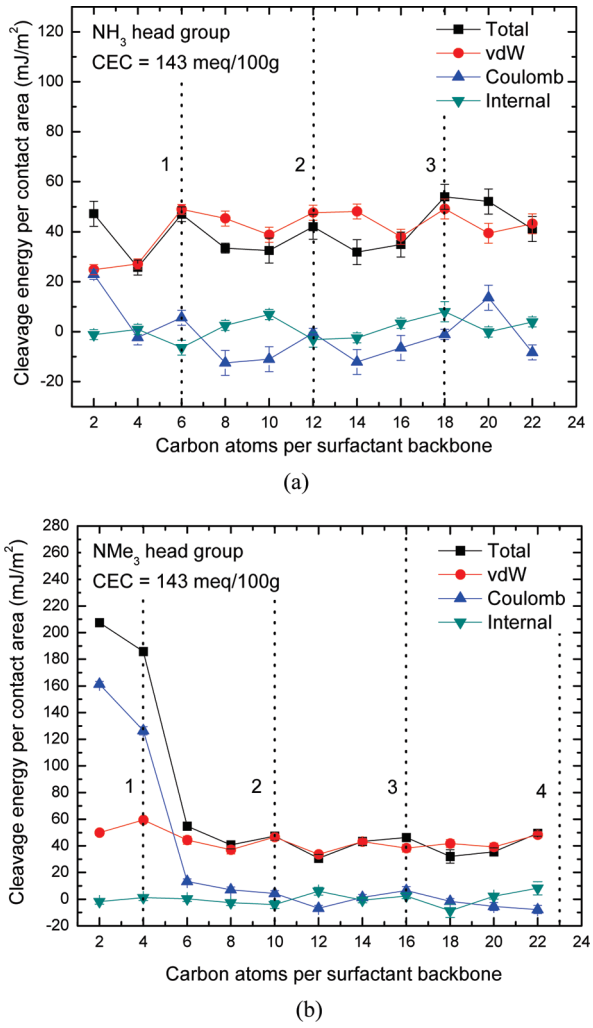

Figure 9. Cleavage energy and additive contributions from Coulomb, van der Waals, and internal interactions for montmorillonite of high CEC (143 meq/100 g) modified with (a) alkylammonium ions with NH_3 head groups and (b) alkylammonium ions with NMe_3 head groups. The vertical lines designated 1, 2, 3, and 4 indicate the chain length corresponding to a densely packed flat-on alkyl monolayer, alkyl bilayer, alkyl trilayer, and alkyl quadrilayer in the interlayer space.

contribution and minimal van der Waals interactions in the partial alkyl bilayer. The cleavage energy reaches a local maximum for the densely packed bilayer at C_{20}, and formation of a partial alkyl trilayer in the interlayer space causes a decrease at C_{22}. We observe high lateral mobility of the head groups for short chains upon cleavage which decreases with increasing chain length (Figure 4).

4.2. Alkylammonium Montmorillonite of High CEC. A high CEC of 143 meq/100 g corresponds to 1.14 cations per nm^2 on a single montmorillonite even surface and a nominal packing density $\lambda_0 = 0.21$ of the alkyl chains.[35] Figure 9 shows the cleavage energy and the additive contributions from Coulomb, van der Waals, and internal energy. We observe a similar sequence of interlayer filling with alkyl chains as a function of chain length as at low CEC; nevertheless, the higher density of head groups per surface area weakens the definition of horizontal alkyl multilayers in the interlayer space through a lower average segmental tilt angle relative to the surface normal.[33,35]

For surfactants with primary ammonium head groups (Figure 9a), cleavage energies amount to between 26 and 54 mJ/m^2 and largely follow the trend in van der Waals energy. Minima occur at 26 mJ/m^2, 32 mJ/m^2, 32 mJ/m^2, and 41 mJ/m^2 for partially packed alkyl monolayers, bilayers, pseudotrilayers, and pseudoquadrilayers in the interlayer space at chain length C_4, C_8 (C_{10}), C_{14}, and C_{22}, respectively. Maxima are found at 47 mJ/m^2 for the shortest surfactant C_2 due to remaining Coulomb contributions as well as at 47 mJ/m^2, 42 mJ/m^2, and 54 mJ/m^2 for densely packed alkyl monolayers, alkyl bilayers, and alkyl pseudotrilayers in the interlayer space at chain length C_6, C_{12}, and C_{18}, respectively. The noticeable Coulomb contribution of 23 mJ/m^2 at chain length C_2 decreases to smaller values for longer chains although fluctuations in Coulomb energy partly account for uncertainties up to ± 5 mJ/m^2 in cleavage energy. van der Waals contributions vary between 25 mJ/m^2 and 49 mJ/m^2 with minima at chain length C_2 (C_4), C_{10}, C_{16}, and C_{20} (C_{22}) for partially packed alkyl monolayers, alkyl bilayers, alkyl trilayers, alkyl quadrilayers, and with maxima at chain length C_6, C_{12}, and C_{18} for densely packed alkyl monolayers, alkyl bilayers, and alkyl trilayers. The gain in van der Waals energy for alkyl chains in densely packed alkyl layers appears to somewhat increase the Coulomb attraction in the unified structure (C_6, C_{12}, and C_{18}/C_{20} in Figure 9a) which contributes to local maxima of the cleavage energy.

For surfactants with quaternary ammonium head groups (Figure 9b), cleavage energies reach a maximum of 200 mJ/m^2 for chain length C_2 and C_4. It follows a minimum of 41 mJ/m^2 for C_8, a maximum at 47 mJ/m^2 for C_{10}, a minimum at 31 mJ/m^2 for C_{12}, a maximum at 46 mJ/m^2 for C_{16}, a minimum at 33 mJ/m^2 for C_{18}, and a maximum at 44 mJ/m^2 for C_{22}. The highest cleavage energy is found for short chains due to vertical sharing of the head groups between the two montmorillonite layers at equilibrium separation and consequently high Coulomb energy (see C_2 at $d = 0$ nm in Figure 6a). The subsequent decrease in cleavage energy upon formation of an alkyl bilayer at chain length C_6 is associated with the vertical separation of the head groups between the two layers and a sharp decrease in Coulomb contributions from 160 mJ/m^2 to < 15 mJ/m^2 (see C_{14} in Figure 6b at $d = 0$ nm). van der Waals contributions to the cleavage energy vary between 34 mJ/m^2 and 59 mJ/m^2 with minima for partially packed alkyl layers at chain length C_8, C_{12}, and C_{18} and maxima for densely packed alkyl layers at chain length C_{10}, C_{16}, and C_{22} in the interlayer space. This trend leads to local minima of the cleavage energy for partially packed alkyl layers for chain length C_8, C_{12}, and C_{18} and local maxima for densely packed alkyl layers for chain length C_{10}, C_{16} (within error), and C_{22}. Notable is also the lateral mobility of the head groups upon cleavage which is greater for short alkyl chains and remains significant for longer alkyl chains (Figure 6).

In summary, the most influential factors for the cleavage energy are the degree of distribution of head groups to individual montmorillonite layers at equilibrium

Table 1. Experimentally Determined Surface Tension γ and Computed Cleavage Energies ε_S (mJ/m^2) for H_3N^+-C_nH_{2n+1} Modified Montmorillonite[f]

chain length	none[c]	C_2	C_4	C_6	C_8	C_{10}	C_{12}	C_{14}	C_{16}	C_{18}	C_{20}	C_{22}
γ (expt)[a]	~60			46.4	44.9	44.9; 43.6[e]	42.3	42.4				
ε_S (sim)[b]	133[d]	36.2	24.6	35.8	46.2	45.3	41.2	32.9	39.1	42.2	51.4	52.4
stddev	±5	±2.5	±3.0	±2.0	±2.0	±2.0	±2.0	±2.1	±2.3	±5.0	±3.0	±3.0

[a] CEC 68 meq/100 g. Data from ref 43. [b] CEC 91 meq/100 g. Data from Figures 7 and 8. Note that cleavage free energies are up to 3 mJ/m^2 lower (see text). [c] Na-montmorillonite without surfactant modification for comparison. [d] Reference 31. [e] Reference 44. [f] In the absence of residual Coulomb contributions, the cleavage energy exhibits fluctuation as a function of the interlayer environment and approximates steady values of the surface tension in the case of densely packed alkyl interlayers.

separation and the interlayer density. Vertically separated head groups and low interlayer density lead to minimal cleavage energy. Head groups not distributed between the two clay layers and high interlayer density lead to maximum cleavage energy. The lateral mobility of alkyltrimethylammonium surfactants upon cleavage is much higher compared to alkylammonium surfactants.

5. Comparison of Cleavage Energy and Surface Tension

Surface tensions and cleavage free energies are different physical quantities since surface tensions are measured on cleaved surfaces in contact with various liquids or vacuum,[41−45] while cleavage free energies depend on the vertical distribution of cationic groups and on the alkyl density in the interlayer space (see section 2.3). Experimental observations[41−45] suggest that a similar environment is seen by liquids in contact angle measurements on various cleaved alkylammonium-modified surfaces as a function of CEC, different head groups, and chain lengths as the surface tension exhibits little variation. This trend is indicated in Table 1 for a series of primary alkylammonium surfactants on the surface of Wyoming montmorillonite with a CEC of 68 meq/100 g.[41−43,45] The experimental CEC is lower than in the models (CEC of 91 meq/100 g) so that layered silicates in the surface tension measurement are best compared to layered silicates with somewhat shorter alkylammonium chains in the simulation of cleavage energies. Nevertheless, the cleavage energies exhibit clear increases and decreases as a function of chain length since surface reconstruction and the interlayer density play a major role (Table 1). Thereby, densely packed interlayer structures appear to better approximate solvated interfaces, and the associated cleavage energies approach the surface tension. Partially packed interlayer structures, in contrast, lead to lower cleavage energy compared to the surface tension. Moreover, cleavage free energies are between 0 and 3 mJ/m^2 (CEC 91 meq/100 g), or between 0 and 5 mJ/m^2 (CEC 143 meq/100 g), lower than cleavage energies as a function of increasing chain length up to C_{22} due to entropy gains upon cleavage.[31]

In addition, a surface tension of 44.2 mJ/m^2 was determined for hexadecyltrimethylammonium-modified Wyoming montmorillonite (CEC 68 meq/100 g)[43] which is somewhat higher than the computed cleavage energy ~42 mJ/m^2 for a C_{12} montmorillonite (CEC 91 meq/100 g), taking into account the difference in CEC (Figure 8b). The corresponding cleavage free energy of ~40 mJ/m^2 is slightly lower than the surface tension as the surfactant structure resembles a loosely packed bilayer.

Surface tensions between 40 and 50 mJ/m^2 were also reported for other quaternary alkylammonium and quaternary alkylphosphonium modified montmorillonites[45] and between 50 and 56 mJ/m^2 for alkylammonium laponite (CEC ~115 meq/100 g).[43] These values coincide with the upper range of cleavage free energies derived from the simulation of longer surfactants with densely packed alkyl layers after entropy corrections (Figure 7).

6. Conclusions

We introduced a thermodynamic model to understand exfoliation in layered silicate-polymer nanocomposites and investigated the cleavage process as well as the cleavage energy of 44 different alkylammonium montmorillonites as a function of CEC, headgroup chemistry, and chain length using molecular dynamics simulation in all-atomic resolution. We find a widely tunable range of cleavage energies between 25 mJ/m^2 and 210 mJ/m^2. Low values of the cleavage energy increase the propensity of exfoliation in hydrophobic polymer matrices. Therefore, nonhydrated, alkylammonium-modified clay minerals of 25 mJ/m^2 to 30 mJ/m^2 cleavage energy may have more promise of exfoliation compared to widely used organically modified montmorillonites with chain lengths between C_{14} and C_{18} and higher cleavage energies of 45 ± 10 mJ/m^2.

Cleavage energies are difficult to determine in experiment, and surface tensions cannot describe thermodynamic trends in layer separation as they relate to cleaved surfaces and do not take into account the presence of specific interlayer environments upon cleavage. To quantify the cleavage energy by simulation, we employed several methods to obtain statistically justified equilibrium configurations (Figure 2) and analyzed the redistribution of head groups and alkyl surfactants on the surface of the organically modified clay minerals. The cleavage energy is determined by the vertical distribution of the head groups between the clay mineral layers at equilibrium separation and by the interlayer density. When the head groups are vertically separated between the two clay mineral layers at equilibrium separation, as is the case for primary ammonium surfactants, Coulomb contributions to the cleavage energy are low and van der Waals interactions in the interlayer determine the cleavage en-

ergy as a function of chain length. Densely packed, flat-on alkyl layers then lead to higher cleavage energy (up to 60 mJ/m^2) and loosely packed alkyl layers to lower cleavage energy (down to 25 mJ/m^2). Low cleavage energies of 25 mJ/m^2 were computed for $C_4H_9NH_3^+$ surfactants at CEC 91 meq/100 g and at CEC 143 meq/100 g, and cleavage energies of $\sim$30 mJ/m^2 were found for partially packed alkyl bilayers in the nonhydrated interlayer space (Figure 7). When the head groups are not vertically separated between two clay mineral layers at equilibrium separation, Coulomb contributions across the interlayer space are high so that cleavage energies exceed 200 mJ/m^2, such as for small quaternary ammonium surfactants at CEC 143 meq/100 g. Coulomb contributions decrease upon formation of a partial alkyl bilayer in the interlayer space, and then cleavage energies mostly correlate with van der Waals energies as a function of interlayer density.

Future challenges include the simulation of layered silicate-polymer interfaces in full atomic resolution and multilevel approaches to cover more broadly the length and time scales.[34] The full analysis of the exfoliation process indicated in Figure 1 and the magnitude of interface tensions across the region between mineral, surfactant, and polymer to specify ΔG and γ_{MP} in eq 3 by simulation could further advance the understanding of thermodynamic and kinetic stability of composites.

Acknowledgment. We are grateful for support by the University of Akron, the Ohio Department of Development, and a generous allocation of computational resources at the Ohio Supercomputing Center. Helpful discussions with Richard Vaia, Air Force Research Laboratory, Wright-Patterson Air Force Base, are acknowledged.

Supporting Information Available: Detailed description of the determination of the total energy of alkylammonium-modified montmorillonite layers in the cleaved and in the unified state, associated uncertainty, and of the suitability of sampling methods I−IV. This material is available free of charge via the Internet at http://pubs.acs.org.